Catalysis Today 146 (2009) 110–123

Contents lists available at ScienceDirect

Catalysis Today

journal homepage: www.elsevier.com/locate/cattod

Hydrogen production from ethanol for PEM fuel cells. An integrated fuel processor comprising ethanol steam reforming and preferential oxidation of CO

Sania M. de Lima [a,1], Rita C. Colman [a], Gary Jacobs [b], Burtron H. Davis [b], Kátia R. Souza [a], Adriana F.F. de Lima [a], Lucia G. Appel [a], Lisiane V. Mattos [a], Fábio B. Noronha [a,*]

[a] Instituto Nacional de Tecnologia - INT, Av. Venezuela 82, CEP 20081-312, Rio de Janeiro, Brazil
[b] Center for Applied Energy Research, The University of Kentucky, 2540 Research Park Drive, Lexington, KY 40511, USA

ARTICLE INFO

Article history:
Available online 10 March 2009

Keywords:
Fuel cell
Fuel processor
Hydrogen production
Steam reforming of ethanol
Preferential oxidation of CO
CO clean up

ABSTRACT

The aim of the work was to study the performance of ceria catalysts to convert ethanol to hydrogen in a combined system including ethanol steam reforming and PROX. The roles of the active oxide component, partially reduced ceria, and the metal component, Pt, in the ethanol steam reforming mechanism were investigated by diffuse reflectance infrared spectroscopy (DRIFTS) carried out under steady state reaction conditions. The main mechanism was found to proceed by (1) dissociative adsorption of ethanol to ethoxy species; (2) dehydrogenation of ethoxy species to adsorbed acetaldehyde; (3) oxidation of acetaldehyde species by ceria OH groups to acetate; (4) acetate demethanation to CH_4 and carbonate species; (5) carbonate decomposition to CO_2; and presumably (6) CH_4 decomposition steps. Though Pt improved the initial ethanol conversion rate by facilitating hydrogen transfer and demethanation steps, the Pt–ceria interface was quickly lost to the buildup of carbon-containing species, thus hindering the Pt from effectively demethanating the acetate intermediate. Unpromoted ceria, though less active, was a significantly more stable catalyst.

The steps for the PROX reaction in the presence of acetaldehyde were found to include: (1) decomposition of acetaldehyde leading to CO and methane; (2) hydrogenation of acetaldehyde producing ethanol; and (3) oxidation of the CO.

© 2009 Elsevier B.V. All rights reserved.

1. Introduction

Nowadays, the absence of a suitable hydrogen distribution infrastructure is one of the main barriers to the use of hydrogen as an energy carrier or as a fuel for energy generation [1,2]. In the early stages of the transition to a hydrogen economy, hydrogen should be produced locally at refueling stations using small-scale fuel processors [3]. These fuel processors pose new challenges for catalyst design as a consequence of their operating conditions and the need for high performance at low cost [4]. Depending on the applications, hydrogen rich streams with very low CO contents (below 10 ppm) are necessary and then further processing steps are required. In this case, the reformer is followed by a clean up step such as the water–gas shift reaction (WGS), CO preferential oxidation (PROX), pressure swing adsorption (PSA) or CO methanation. The selection of the different stages of the fuel processor affects significantly the efficiency and the cost of the fuel processor [5]. Different approaches have been proposed to reduce the complexity of the fuel processor such as the use of membrane reactors, which integrates the reaction and the separation steps within the same reactor, or the development of new catalysts designed specifically for the small-scale processors [4]. They must be active, selective to hydrogen and stable under the reaction conditions.

For example, a fuel processor to generate hydrogen from ethanol is a rather attractive technology since ethanol is a renewable raw material obtained from fermentation of various agricultural products (e.g., sugar cane). This light alcohol is a high energy density carrier for hydrogen and can be more easily transported by vehicle or pumped to a point of use, where it can be reformed to release the hydrogen with a fuel processor. However, the development of suitable catalysts to effect this reaction is proving to be a challenge. In the literature, the majority of authors [6–15] reported using supported metals as catalysts for the ethanol reforming

* Corresponding author at: Instituto Nacional de Tecnologia - INT, Catalysis Laboratory, Av. Venezuela 82, CEP 20081-312, Rio de Janeiro, Brazil.
Tel.: +55 21 2123 1177; fax: +55 21 2123 1051.
E-mail address: fabiobel@int.gov.br (F.B. Noronha).
[1] Present address: Universidade Estadual do Oeste do Paraná - Unioeste, Campus de Toledo, Rua da Faculdade, 645, Jd. La Salle, CEP 85903-000, Toledo, Brazil.

0920-5861/$ – see front matter © 2009 Elsevier B.V. All rights reserved.
doi:10.1016/j.cattod.2009.02.006

reactions. In general, these catalysts exhibited optimal performance at high temperatures (between 873 and 1023 K) and consequently, large amounts of CO were formed, which increases the fuel processor cost, due to the added complexity of the downstream CO conversion process. In addition, catalyst deactivation due to carbon deposition is an important issue [16–18]. A different catalyst design approach is to use metal oxides as catalysts for steam reforming of ethanol [19–22]. In spite of their lower activity than supported metal catalysts, metal oxides are capable of producing hydrogen free of CO as well as carbon deposits, depending on the reaction conditions used. This may eliminate some purification steps and as a result reduce the costs. However, a wide range of undesirable by-products (e.g., ethene, acetaldehyde and acetone) is formed during steam reforming of ethanol over metal oxides in comparison with supported metal catalysts. For instance, acetaldehyde produced upstream may impact the performance of the downstream PROX catalyst. Therefore, the design of an appropriate catalyst that can handle both the reforming as well as the purification steps would go a long way to improve the overall efficiency of the fuel processor.

Ceria and ceria-containing mixed oxides have been proposed as catalytically active components for ethanol conversion reactions due to their high oxygen storage capacity, which improves catalyst stability [23–27]. In addition, the strong metal–support interaction prevents metal particle sintering, which also contributes to catalyst deactivation. Recently, we have investigated the performance of supported Pt catalysts for steam reforming of ethanol [26,27]. At low reaction temperature, the $Pt/CeZrO_2$ catalyst underwent significant deactivation during ethanol decomposition and steam reforming reactions. Co-feeding oxygen decreased the deactivation rate of the catalyst but adversely impacted the selectivity to hydrogen. Increasing the reaction temperature greatly improved the stability of the catalyst [26]. A reaction mechanism was proposed based upon results obtained from in situ diffuse reflectance infrared spectroscopy (DRIFTS) analyses carried out under reaction conditions. The effect of the support nature and metal dispersion on the performance of supported Pt catalysts during steam reforming of ethanol was also studied [27]. H_2 and CO production were facilitated over Pt/CeO_2 and $Pt/CeZrO_2$, whereas the acetaldehyde and ethene formation were favored on Pt/ZrO_2. However, regardless of the support used, all the catalysts significantly deactivated during the reaction at low temperature. Unpromoted cerium oxide has also been used as a catalyst for the steam reforming of ethanol [19,20,22]. CeO_2 exhibited activity for steam reforming of ethanol while CO was not detected or it was formed in very low concentrations.

Many catalysts have been considered for the PROX reaction. A recent work published by Park et al. [28] describes an overview of the performance of many catalytic systems, including Au, Pt, Cu, Rh and Ru supported on different oxides. However, as far as we know in the literature, there is no data related to the impact of oxygenates on the catalytic performance of the PROX reaction.

The aim of this work is to study the performance of catalysts used to convert ethanol to hydrogen in a combined system including steam reforming and PROX reactions. CeO_2 and Pt/CeO_2 catalyst were tested for the steam reforming of ethanol and the role of the support on the reaction mechanism was investigated using diffuse reflectance infrared spectroscopy carried out under steady state reaction conditions. Attention was also focused on the activity of Pt/CeO_2 catalysts for CO and acetaldehyde removal.

2. Experimental

2.1. Catalyst preparation

CeO_2 and Al_2O_3 were used as supports. Al_2O_3 was supplied by NORPRO and CeO_2 support was obtained by calcination of $(NH_4)_2Ce(NO_3)_6$ in a muffle furnace at 1073 K for 1 h.

Platinum was added to the supports by the incipient wetness impregnation technique using an aqueous solution of $H_2PtCl_6{\cdot}6H_2O$. After impregnation, the samples were dried at 393 K and calcined under air flow (50 mL/min) at 673 K for 2 h. The following catalysts were obtained: 0.5%Pt/CeO_2, 1.0%Pt/CeO_2, 1.5%Pt/CeO_2, 2.0%Pt/CeO_2 and 1.5% Pt/Al_2O_3.

2.2. BET surface area

The BET surface areas were measured using a Micromeritics ASAP 2000 analyzer by nitrogen adsorption at the boiling temperature of liquid nitrogen.

2.3. Temperature Programmed Reduction (TPR)

Temperature Programmed Reduction measurements were carried out in a micro-reactor coupled to a quadrupole mass spectrometer (Balzers, Omnistar). The samples (300 mg) were dehydrated at 423 K for 30 min in a He flow prior to reduction. After cooling to room temperature, a mixture of 5% H_2 in Ar flowed through the sample at 30 cm^3/min, raising the temperature at a heating rate of 10 K/min up to 1273 K.

2.4. Cyclohexane dehydrogenation

Platinum dispersion was estimated through cyclohexane dehydrogenation, a structure-insensitive reaction [29]. Since H_2 and CO spillover occurs over a CeO_2 support, metal dispersion could not be determined from the chemisorption of both gases [30]. To estimate the dispersion of the Pt/CeO_2 catalysts, a correlation between the rate of cyclohexane dehydrogenation and the metal dispersion measured by hydrogen chemisorption was established from Pt/Al_2O_3 catalysts with different metal particle sizes.

Cyclohexane dehydrogenation was performed in a fixed-bed reactor at atmospheric pressure. The catalysts (50 mg) were reduced at 623 K for 1 h, and the reaction was carried out at 543 K and WHSV = 170 h^{-1}. The reactants were fed to the reactor by bubbling H_2 through a saturator containing cyclohexane kept at 285 K, with the intention of obtaining the desired H_2/HC ratio (13:1). The exit gases were analyzed by on-line gas chromatography.

2.5. Temperature Programmed Desorption (TPD) of ethanol

TPD experiments of adsorbed ethanol were carried out in a micro-reactor coupled to a quadrupole mass spectrometer (Omnistar, Balzers). Prior to TPD analyses, the samples were reduced under flowing H_2 (30 mL/min) ramping the temperature at a rate of 10 K/min to 773 K, and holding at this temperature for 1 h. After reduction, the system was purged with helium at 773 K for 30 min and cooled to room temperature. The adsorption of ethanol was carried out at room temperature using an ethanol/He mixture, which was obtained by flowing He through a saturator containing ethanol at 298 K. After adsorption, the catalyst was heated at 20 K/min to 773 K under flowing helium (60 mL/min). The products were monitored using a quadrupole mass spectrometer.

2.6. DRIFTS

DRIFTS spectra were recorded using a Nicolet Nexus 870 spectrometer equipped with a DTGS-TEC detector. A Thermo Spectra-Tech cell capable of high pressure/high temperature operation and fitted with ZnSe windows served as the reaction chamber for in situ adsorption and reaction measurements. Scans

were taken at a resolution of 4 to give a data spacing of 1928 cm^{-1}. Depending on the signal-to-noise ratio, the number of scans ranged from 256 to 1024. The amount of catalyst was ~40 mg.

Samples were first reduced by ramping in 200 mL/min H_2:He (1:1) at ~10 K/min and holding at 773 K for 1 h. The catalyst was purged in flowing He at 773 K, prior to cooling in flowing He to 313 K.

For ethanol adsorption and ethanol steam reforming reaction tests, He was bubbled at ~15 mL/min through a saturator filled with ethanol and held at 273 K. For ethanol steam reforming tests, a second helium stream (~15 mL/min) was bubbled through a saturator filled with water and held at 298 K. The two streams were joined at a tee-junction, prior to which 1 psig check valves were placed on the lines to prevent a back-flow condition. The saturator gas flows and temperatures were set to provide a H_2O:CH_3CH_2OH stoichiometric ratio of 2:1, which is nominal for SR. Adsorption/reaction measurements were started in the range of 313–323 K, and then the temperature was increased at 10 K/min; measurements were recorded at 373, 473, 573, 673 and 773 K. To explore the deactivation of the catalyst, the changes in spectra were monitored as a function of time onstream by flowing the ethanol/H_2O mixture at 773 K for approximately 6 h.

2.7. Reaction conditions

2.7.1. Ethanol decomposition and steam reforming of ethanol

Ethanol decomposition (i.e., H_2O/ethanol molar ratio = 0.0) was carried out on unpromoted CeO_2. Steam reforming of ethanol was performed over unpromoted CeO_2 and 1.5%Pt/CeO_2 catalyst. All reactions were carried out in a fixed-bed reactor at atmospheric pressure. To activate the catalyst, the samples were reduced under flowing H_2 at 773 K for 1 h and then purged with N_2 at the same temperature for 30 min. Ethanol decomposition and steam reforming of ethanol reactions were carried out at 773 K. For steam reforming of ethanol, H_2O/ethanol molar ratios of 2.0, 3.0 or 5.0 were utilized. The reactant mixtures were obtained using two saturators containing water and ethanol, which were maintained at the temperature required to obtain the desired H_2O/ethanol molar ratios. For ethanol decomposition, N_2 (30 mL/min) was passed through the saturator with ethanol, and then the reactant mixture obtained was diluted with N_2 (30 mL/min). In the case of steam reforming, the reactant mixture was obtained by flowing two N_2 streams (30 mL/min) through each saturator containing ethanol and water separately. The partial pressure of ethanol was maintained constant for all experiments. The variation of partial pressure of water was compensated by a decrease in the partial pressure of N_2. In order to explore the catalyst deactivation within a short period of time, a small amount of catalyst was used (20 mg). The samples were diluted with inert SiC (SiC mass/catalyst mass = 3.0). The reaction products were analyzed by gas chromatography (Micro GC Agilent 3000 A) with the instrument containing two channels for dual thermal conductivity detectors (TCD) and two columns: a molecular sieve and a Poraplot U column.

The ethanol conversion and product selectivities were determined from

$$X_{\text{ethanol}} = \frac{(n_{\text{ethanol}})_{\text{fed}} - (n_{\text{ethanol}})_{\text{exit}}}{(n_{\text{ethanol}})_{\text{fed}}} \times 100 \quad (1)$$

$$S_{\text{x}} = \frac{(n_{\text{x}})_{\text{produced}}}{(n_{\text{total}})_{\text{produced}}} \times 100 \quad (2)$$

where $(n_x)_{produced}$ = moles of x produced (x = hydrogen, CO, CO_2, methane, acetaldehyde or ethene) and $(n_{total})_{produced}$ = moles of H_2 + moles of CO + moles of CO_2 + moles of acetaldehyde + moles of ethene (the moles of water produced are not included).

2.7.2. Preferential oxidation of CO

The catalytic tests were performed in a fixed-bed reactor, monitored by on-line gas chromatography, equipped with flame ionization and conductivity detectors and also a methanator. Before each run, the catalysts were reduced under flowing H_2 (30 mL/min) at 623 K during 30 min. Three different experiments were carried out: (i) the reaction was performed at 348 K by using 8 mg of catalyst and a reactant mixture containing 50% H_2, 200 ppm CO, 2% O_2 and balanced with N_2 in order to measure the rate of CO consumption; (ii) the catalyst (15 mg) performance was evaluated in the temperature range of 325–525 K, in 25 and 50 K increments. The catalyst was held at each temperature for at least 2 h. The composition of the reactant mixture was 50% H_2, 200 ppm CO, 2% O_2 and 0–1% acetaldehyde balanced with N_2; (iii) the reaction of acetaldehyde in absence of oxygen was carried out using 200 mg of catalyst and a reactant mixture containing 61% H_2 and 3.7% of acetaldehyde balanced with N_2.

3. Results and discussion

3.1. Catalyst characterization

The BET surface area of CeO_2 support was very low (14 m^2/g) and it was not measurably affected by the addition of platinum. Alumina exhibited a BET surface area of 200 m^2/g. The Pt dispersion values obtained were 58 and 80% for 1.5%Pt/CeO_2 and 1.5%Pt/Al_2O_3 catalyst, respectively.

The TPR profiles of CeO_2 and 1.5%Pt/CeO_2 are presented in Fig. 1. For the CeO_2, a small H_2 uptake at 817 K and a strong H_2 consumption at 1230 K were observed. The first peak is attributed to the surface reduction of CeO_2 and the second one to the formation of Ce_2O_3 [31]. The TPR profile of the 1.5%Pt/CeO_2 catalyst presented two peaks at 457 and 1256 K, respectively. The former corresponds not only to the PtO_2 reduction but also to CeO_2 surface

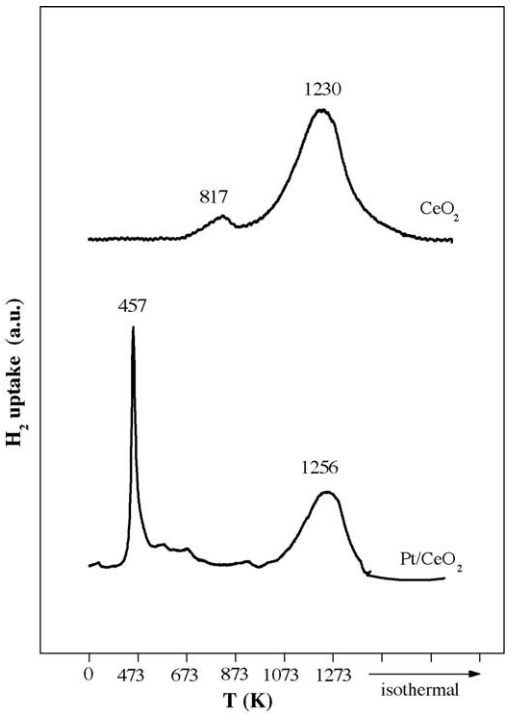

Fig. 1. Temperature Programmed Reduction profiles of CeO_2 and 1.5%Pt/CeO_2.

reduction. The peak at 1256 K is ascribed to bulk CeO_2 reduction [31]. A comparison between the TPR profiles of supports and catalysts shows that the addition of Pt promotes the reduction of support. This promoting effect is due to the hydrogen spillover from metal particles onto the support.

3.2. Steam reforming of ethanol over unpromoted CeO_2 and 1.5%Pt/CeO_2

Ethanol conversion and product distributions as a function of time on stream (TOS) obtained for unpromoted CeO_2 and 1.5%Pt/CeO_2 during steam reforming of ethanol with H_2O/ethanol molar ratio of 2.0 at 773 K are presented in Fig. 2a and b, respectively. 1.5%Pt/CeO_2 catalyst exhibited the highest initial ethanol conversion. However, this catalyst significantly deactivated during the reaction, whereas unpromoted CeO_2 was quite stable, after an initial transient period. Further discussion of the 1.5%Pt/CeO_2 catalyst deactivation is presented (Section 3.5) in terms of the proposed mechanism following the analysis of DRIFTS.

Regarding the product distributions, hydrogen, CO_2 and ethene were the main products obtained over unpromoted CeO_2. Small quantities of acetaldehyde (around 3%) and trace amounts of methane were also observed. It is important to stress that the production of CO during testing of the unpromoted CeO_2 catalyst was very low (less than 200 ppm). This result reduces significantly the complexity of the fuel processor, since the water gas shift reaction step of the fuel processor is no longer needed, decreasing the costs associated with CO conversion during hydrogen purification.

In the case of 1.5%Pt/CeO_2 catalyst, at the beginning of the reaction, the main products observed were hydrogen, methane and CO_2. In addition, small quantities of CO (around 6%) and trace amounts of acetaldehyde were also detected. Nevertheless, as the catalyst deactivated, the acetaldehyde and CO_2 selectivities increased while the hydrogen, methane and CO selectivities decreased. A decrease in H_2 selectivity and an increase in the acetaldehyde selectivity during steam reforming of ethanol over an alumina-supported Pt catalyst were also detected by Dömök et al. [32].

In order to study the effect of the addition of the noble metal to the oxide on the product distribution, the results obtained on a dry basis at the same level of conversion (60%) and the same reaction conditions (reaction temperature = 773 K and H_2O/ethanol molar ratio = 2.0) for 1.5%Pt/CeO_2 and CeO_2 were evaluated (Table 1). The addition of the metal favored methane and CO formation. On the other hand, ethene production was predominant over unpromoted CeO_2.

Table 1
Product distributions obtained on a dry basis at the same level of conversion (around 60%) during steam reforming of ethanol on CeO_2 support and 1.5Pt/CeO_2 catalyst (reaction temperature = 773 K and H_2O/ethanol molar ratio = 2.0).

Sample	Product distribution (%)					
	H_2	CH_4	CO	CO_2	Acetaldehyde	Ethene
CeO_2	69	0.6	–[a]	14	3.5	13
1.5Pt/CeO_2	63	11	7.5	15	3.0	0

[a] CO concentration <200 ppm.

Since the highest stability and the lowest CO production rates were obtained for unpromoted CeO_2, the performance of this catalyst during ethanol reforming was evaluated in greater detail.

3.3. Effect of the addition of water on the performance of CeO_2 support

In order to study the effect of water addition during ethanol reforming over unpromoted CeO_2, the reactions were carried out at 773 K, using H_2O/ethanol molar ratios of 0.0 (ethanol decomposition), 2.0, 3.0 or 5.0.

Fig. 3a shows the ethanol conversion and product distributions obtained for CeO_2 support during ethanol decomposition. The ethanol conversion was almost complete and it was quite stable during 6 h TOS. Increasing H_2O/ethanol molar ratio from 2.0 (Fig. 2a) to 5.0 (Fig. 3b and c), decreased the initial ethanol conversion rate. This result indicates that ethanol and water compete for the same actives sites. In addition, after an initial transient period, ethanol conversion remained relatively stable under different H_2O/ethanol molar ratios.

Regarding the product distributions, the main products obtained were hydrogen, CO_2 and ethene at all H_2O/ethanol molar ratios studied (Figs. 2 and 3a–c). Small quantities of acetaldehyde (around 2–6%) and trace amounts of methane and CO (less than 200 ppm) were also observed. In the case of ethanol decomposition, a slight decrease in ethene selectivity was accompanied by a small, but measurable increase in H_2 selectivity. However, in the presence of water, no significant changes in the product distribution were observed.

A comparison between the results presented in Fig. 3a (ethanol decomposition) and Fig. 2a (steam reforming with H_2O/ethanol molar ratio = 2.0) showed that although the addition of water did not have a beneficial effect on ethanol conversion, it increased the

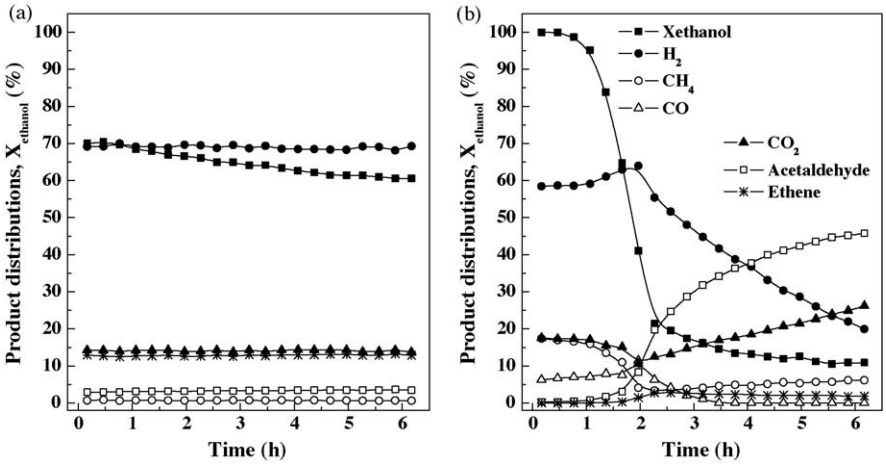

Fig. 2. Ethanol conversion ($X_{ethanol}$) and product distributions versus time on stream obtained during steam reforming of ethanol over (a) unpromoted CeO_2 and (b) 1.5%Pt/CeO_2 catalyst ($T_{reaction}$ = 773 K; H_2O/ethanol molar ratio = 2.0 and residence time = 0.02 g s/mL).

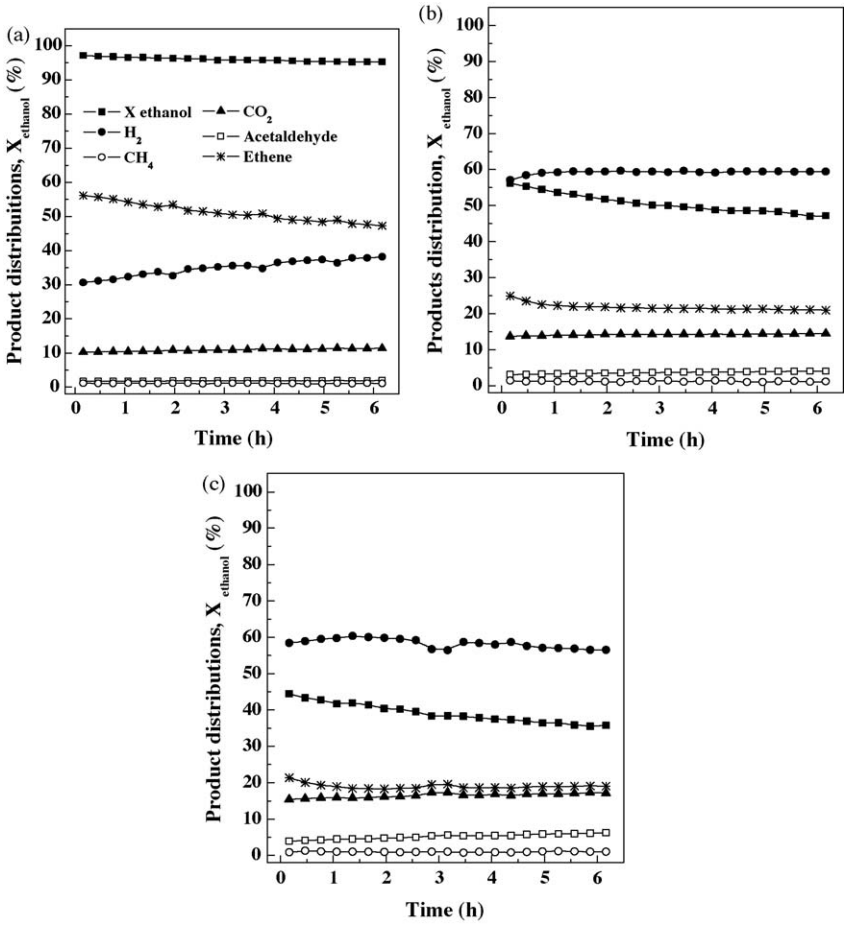

Fig. 3. Ethanol conversion ($X_{ethanol}$) and product distributions versus time on stream obtained during (a) ethanol decomposition (H_2O/ethanol molar ratio = 0.0) and steam reforming of ethanol at H_2O/ethanol molar ratios of (b) 3.0 and (c) 5.0 over unpromoted CeO_2 ($T_{reaction}$ = 773 K and residence time = 0.02 g s/mL).

H_2 and CO_2 selectivities and decreased the acetaldehyde and ethene selectivities. These results indicate that the presence of water in the feed favored the ethanol steam reforming reaction pathway over either the direct ethanol dehydrogenation to acetaldehyde or ethanol dehydration to ethene reaction routes. These results are consistent with the findings of Dömök et al. [32], who reported that increasing the H_2O/ethanol molar ratio led to a decrease in ethene production during steam reforming of ethanol over alumina-supported Pt catalysts. As described above, the presence of water inhibits the dehydration of ethanol pathway, thereby limiting the amount of ethene produced.

3.4. Reaction mechanism of ethanol reforming

3.4.1. TPD of ethanol

The TPD profiles of adsorbed ethanol over unpromoted CeO_2 are shown in Fig. 4a. A peak corresponding to molecular ethanol desorption was observed at 387 K. Several authors [14,33] have detected ethanol adsorption in TPD of ethanol over supported metal catalysts at low temperatures.

Besides ethanol, small amounts of methane and acetaldehyde were also detected around 380 K. Some authors reported that the formation of methane and CO in the low-temperature region during TPD of ethanol could be attributed to the decomposition of ethoxy species formed by the dissociative adsorption of ethanol on the catalyst surface [26,33–37], an explanation that fits well with our observations. The absence of CO suggests that it reacts with the oxygen from the support, present either as adsorbed –O* adatoms or –OH* hydroxyl groups, to form carbonate and/or formate species. Actually, TPR analysis of unpromoted CeO_2 revealed the surface reduction of ceria, at temperatures below 773 K. In addition, the sample was treated for 1 h in H_2 at 773 K, which should favor the conversion of –O* to –OH*. In short, CO reacts with the adsorbed O (present either as –O* or –OH*) to produce associated species that in turn decompose at higher temperature to liberate CO_2.

In the case of acetaldehyde, some authors have shown [14,26] that the formation of acetaldehyde during TPD of ethanol over supported metal catalysts was assigned to direct ethanol dehydrogenation. In addition, the absence of hydrogen desorption in our work suggests that hydrogen still remained adsorbed in the low-temperature region.

At temperatures between 500 and 650 K, a number of products, including hydrogen, methane, CO and ethene were detected. Formation of hydrogen, methane and CO could be related to the decomposition of dehydrogenated species (acetaldehyde and acetyl species) [33,35,36]. Ethene production, on the other hand, is typically assigned to the dehydration of ethanol [14,26].

Above 700 K, hydrogen, CO, CO_2 and methane were formed, and can be assigned to the decomposition of acetate species [33,35,36], a process that in part involves carbonate species as intermediates. Finally, the production of hydrogen detected at high temperature in the TPD profiles of unpromoted CeO_2 can be attributed to the desorption of hydrogen previously formed during the different dehydrogenation steps taking place in the catalysis.

Fig. 4b presents the TPD profiles of adsorbed ethanol for the 1.5%Pt/CeO_2 catalyst. The results obtained were similar to those observed by Mattos and Noronha [33] during TPD of ethanol over CeO_2 supported platinum catalyst.

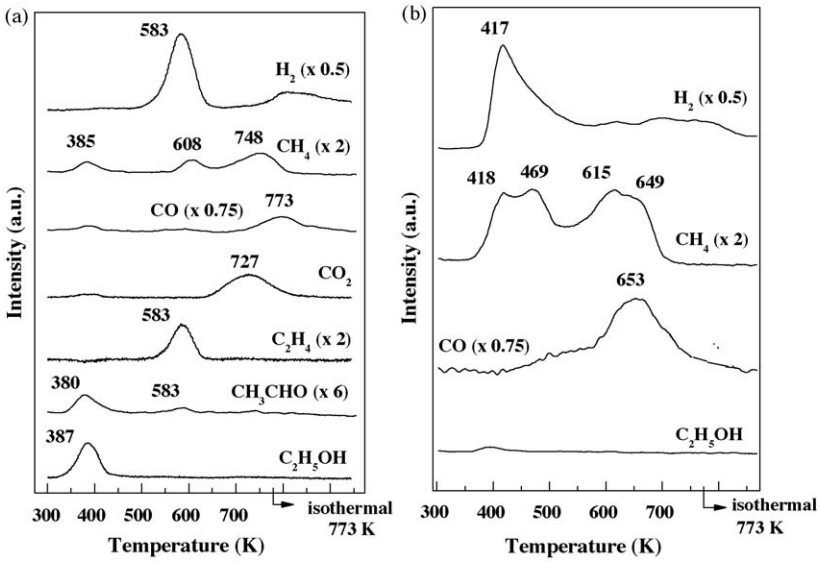

Fig. 4. TPD profiles of ethanol desorption obtained for (a) unpromoted CeO_2 and (b) 1.5%Pt/CeO_2 catalyst.

In contrast to the results obtained for unpromoted CeO_2, no significant desorption profiles of ethanol or acetaldehyde were detected in the low-temperature range over 1.5%Pt/CeO_2 catalyst. On the other hand, 1.5%Pt/CeO_2 catalyst exhibited a significant hydrogen desorption peak (at 417 K) as well as peaks for methane (at 418 and 469 K), which can be attributed to the decomposition of ethoxy species [33–37]. However, according to the literature [33–37], the decomposition of these species produces hydrogen, methane and CO. Then, in this work, the absence of CO desorption suggests that CO remained adsorbed over 1.5%Pt/CeO_2 catalyst at low temperature.

At temperatures above 500 K, a significant TPD peak for CO was detected at 653 K, whereas methane emanated from the surface in two distinct peaks situated at 615 and 649 K, respectively. As described earlier for the case of unpromoted ceria, CO and methane formation in the high-temperature region can be attributed to the conversion of acetate species. In addition, a relatively small desorption peak for hydrogen, previously formed during the various dehydrogenation steps, was observed beginning at approximately 650 K.

By comparing the TPD profiles of unpromoted CeO_2 and 1.5%Pt/CeO_2, a number of differences become apparent. In the low-temperature region (i.e., <490 K), molecular ethanol desorption was only observed with unpromoted CeO_2 support, indicating that 1.5%Pt/CeO_2 possesses a greater density of strong active sites, making the catalyst more active. Furthermore, the formation rates of methane and hydrogen were much higher for the case of the 1.5%Pt/CeO_2 catalyst, suggesting that the decomposition reaction of ethoxy species was promoted by the presence of the metal. However, it is apparent that the CO formed during ethoxy decomposition remained adsorbed on the metal surface, as it was not detected in the gas phase at low temperatures.

At high temperature, both CeO_2 and 1.5%Pt/CeO_2 produced methane and CO, indicating that the decomposition of acetaldehyde and/or acetate species occur in both cases, clearly delineating the role of the oxide in providing adsorption sites for these oxygenate species. However, since the amounts formed were higher over the Pt-containing catalyst, it is apparent that these reactions are promoted by the presence of the Pt metal, indicating that Pt operates on the molecules adsorbed on the ceria itself, at the metal–oxide interface. In addition, CO_2 was only detected over unpromoted CeO_2. As described above, the formation of CO_2 was assigned to the decomposition of carbonate species, which are formed during the conversion of acetate species. Since the TPR profiles of unpromoted CeO_2 and 1.5%Pt/CeO_2 revealed that Pt facilitated reduction of the surface shell of ceria to much lower temperatures, a higher density of oxygen vacancies in the ceria fraction of 1.5%Pt/CeO_2 may provide sites for the CO_2 to react, yielding CO.

It is important to note that, while the TPD studies do provide useful information regarding the impact of Pt addition to ceria, the technique has some limitations. One important drawback is that co-fed water was not present during TPD. The role of co-fed H_2O on promoting the decomposition rates and selectivities of adsorbed species during catalytic reactions has been well documented [10]. This is one reason why water co-feeding was included during the DRIFTS investigations.

3.4.2. DRIFTS analysis of ethanol desorption

Fig. 5 presents DRIFTS spectra of adsorbed ethanol on CeO_2 support at different temperatures. At room temperature, the bands at 1049 and 1099 cm^{-1} correspond to different vibrational modes of ethoxy species, which were formed by dissociative adsorption of ethanol [33–37] and adsorb over Ce cations in bidentate and monodentate modes [38]. The ethoxy species are associated with Ce^{3+} atoms on the surface of ceria consistent with surface shell reduction, which in H_2 flow generates defect-associated Type II bridging OH groups [10]. Since the TPR profile for unpromoted CeO_2 revealed that the surface shell reduction occurs in the 660–880 K range, the 1 h activation at 773 K in H_2 should allow this partial reduction of ceria to take place. Then, the ethoxy species may preferentially adsorb over Ce^{3+} according to Scheme 1.

Besides the bands related to ethoxy species, the DRIFTS spectrum of unpromoted CeO_2 obtained at room temperature exhibited bands at 1306, 1423 and 1562 cm^{-1}, which are assigned to $\delta_s(CH_3)$, $\nu_s(OCO)$, $\nu_a(OCO)$ vibrational modes of acetate species, respectively. The bands at 2863, 2927 and 2971 cm^{-1} are also associated with the different vibrational modes (i.e., C–H stretching) of ethoxy species and acetate species [33]. The presence of the bands assigned to acetate species indicates that ethoxy species were somehow oxidized to acetate species. According to the literature [39,40], ethoxy species are dehydrogenated to acetaldehyde, which may in turn be further dehydrogenated to acetyl species. The acetate species can be formed by two different routes [14]: (i) the reaction between acetaldehyde and surface OH groups and/or (ii) the reaction between the acetyl species and the oxygen

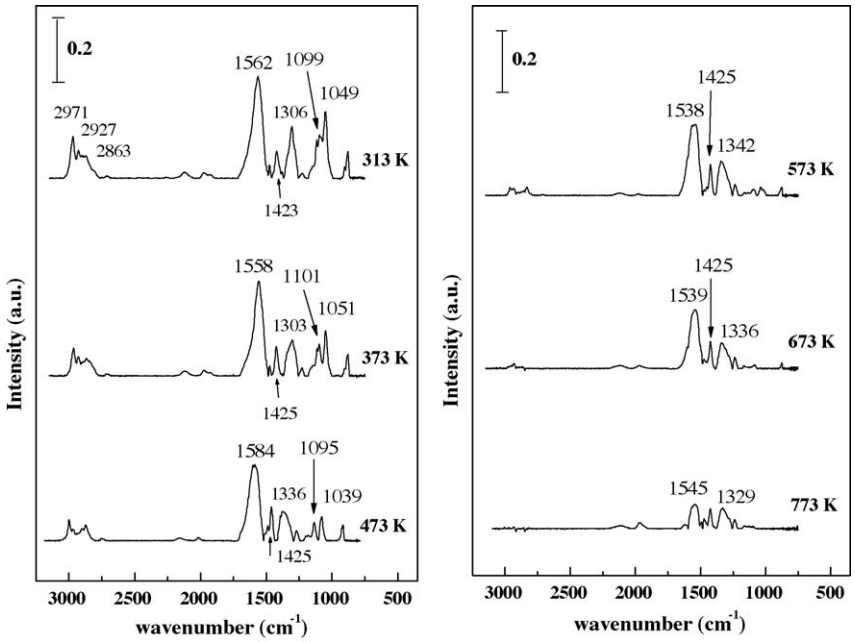

Fig. 5. DRIFTS spectra of adsorbed ethanol obtained at different temperatures for unpromoted CeO_2.

from the support. In the present work, the density of O* adatoms available for reaction should be low over unpromoted CeO_2, since the reduction of the surface shell of ceria should be complete at 773 K in H_2 treatment. Therefore, the route involving the reaction between the ethoxy species (and proposed adsorbed intermediary acetaldehyde) and the surface hydroxyl groups from the support (Scheme 2) may be favored over unpromoted CeO_2 pretreated in H_2 at 773 K.

Increasing the temperature to 373 K, decreased the intensity of the bands corresponding to ethoxy species (1051 and 1101 cm^{-1}) whereas no significant changes were detected in the intensity of the bands assigned to acetate species (1303, 1425 and 1558 cm^{-1}). This result confirms that the methane desorption observed in TPD profiles of unpromoted CeO_2 around 380 K was due to the decomposition of a fraction of ethoxy species.

When unpromoted CeO_2 was heated to 673 K, the bands associated with ethoxy species were no longer detected while those assigned to acetate species decreased. In addition, the absence of bands at 2860–2970 cm^{-1} suggests that carbonate species are formed at high temperatures on CeO_2. Nevertheless, the presence of the acetate species may not be ruled out, since it is very hard to distinguish between carbonate species and acetate species by the vibrational modes in the O–C–O stretching region [33]. Above 673 K, the bands corresponding to acetate species and/or carbonate species significantly decreased. Comparing this result and TPD experiments for unpromoted CeO_2, it is clear that the acetate species decomposed to CH_4 and CO_X over the active oxide surface at high temperature.

The DRIFTS spectrum for the adsorption of ethanol over 1.5%Pt/CeO_2 catalyst at room temperature (Fig. 6) also exhibited bands assigned to ethoxy species (1041, 1080 and 1406 cm^{-1}), acetate species (1319, 1450 and 1562 cm^{-1}), as well as bands assigned to both ethoxy and acetate species (2902, 2955 and 2974 cm^{-1}). The TPR analysis showed that the degree of the reduction of ceria surface shell of the catalyst is higher than that obtained for unpromoted ceria below 773 K, indicating that the ethoxy species are adsorbed over Ce^{3+} cations (i.e., oxygen vacancy defects). In addition, the formation of ethoxy species from the adsorption of ethanol over Ce^{3+} cations occurs simultaneously with the formation of hydroxyl groups by dissociation of the ethanol molecule. During ethanol adsorption, a decrease in a band at ~3650 cm^{-1} indicates that the ethanol adsorption displaces H_2O that was dissociated at O vacancies according to a mechanism previously reported by de Lima et al. [26,27]. In the case of acetate species formation, since the surface of the catalyst has been partially reduced by the hydrogen treatment, the density of O* adatoms available for reaction should be at least low and possibly lower than that obtained for unpromoted CeO_2. Therefore, the route from ethoxy to acetate involving OH is likely. This mechanism was proposed by de Lima et al. [26] during DRIFTS of ethanol desorption over Pt/$CeZrO_2$ catalyst, whose ceria surface was completely reduced by hydrogen. According to them, after the reduction, the density

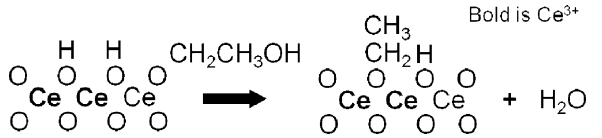

Scheme 1. Activation of ethanol on Ce^{3+} cations by ethoxy formation.

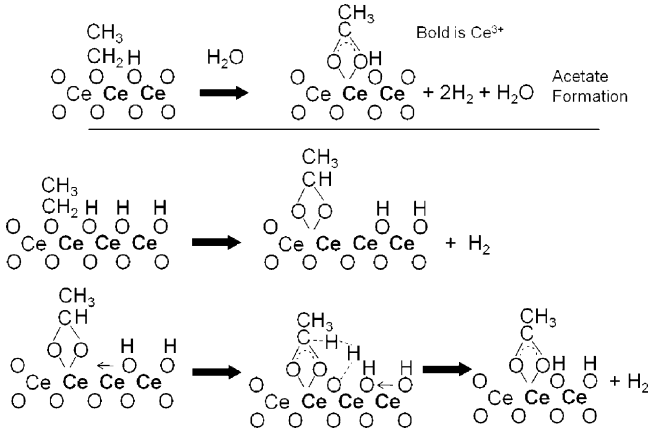

Scheme 2. Transformation of ethoxy to acetate species by surface oxygen present in the form of bridging OH groups over partially reduced ceria.

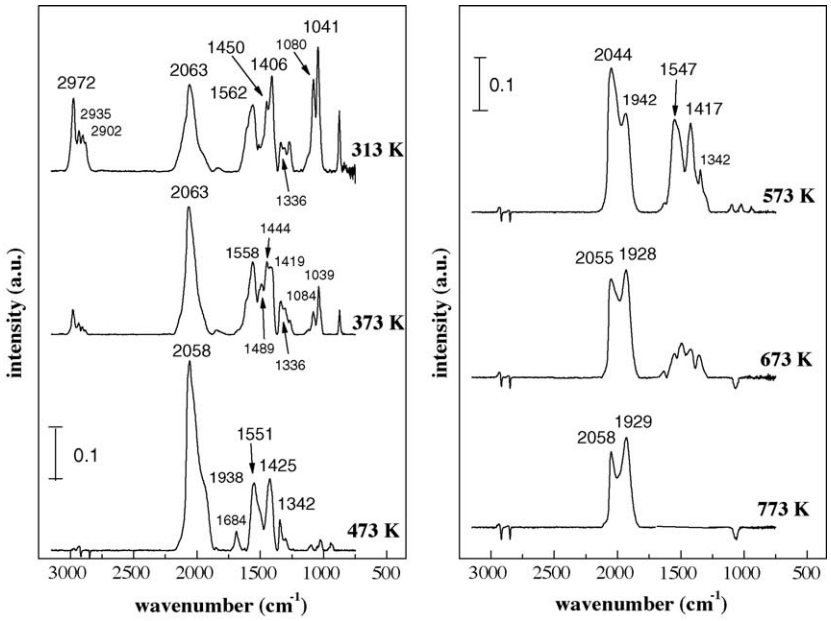

Fig. 6. DRIFTS spectra of adsorbed ethanol obtained at different temperatures for 1.5%Pt/CeO_2 catalyst.

of O* adatoms available for reaction over Pt/$CeZrO_2$ catalyst should be low relative to the adsorbed OH* group and, therefore the route from ethoxy to acetate involving Type II bridging OH groups appears to be more likely.

In addition to the bands assigned to ethoxy and acetate species, the spectrum of 1.5%Pt/CeO_2 also exhibited a band attributed to the ν(CO) mode of linearly adsorbed CO on small Pt particles (2063 cm^{-1}) [26,41–43].

When the 1.5%Pt/CeO_2 catalyst was heated to 373 K, the intensity of the bands corresponding to ethoxy species decreased whereas the intensity of the bands assigned to CO adsorbed on metal particles increased. In addition, the bands related to acetate species remained unchanged. The decrease in the intensities of bands corresponding to ethoxy species and the increase of those associated with CO formation confirm that ethanol decomposes to CO, methane and hydrogen.

At 473 K, the bands associated with ethoxy species completely disappeared whereas those assigned to acetate species slightly increased. A significant increase in the intensities of the bands corresponding to CO (2058 cm^{-1}) was also observed. In addition a shoulder at 1938 cm^{-1} is now detected, which corresponds to the ν(CO) mode of bridged CO bound to large Pt particles. These results are consistent with the TPD of adsorbed ethanol (Fig. 4b), which revealed desorption of methane and hydrogen between 418 and 469 K. The increase of the CO band and the corresponding decrease of the bands for ethoxy species confirm that the decomposition of ethoxy species occurs in the low-temperature region and that CO formed remained adsorbed on the Pt component of the catalyst. de Lima et al. [26] reported similar results during DRIFTS of ethanol desorption over Pt/$CeZrO_2$ catalyst. Dömök et al. [32] monitored by mass spectrometry the gas phase composition during IR experiments. Their results indicated the formation of hydrogen and methane, confirming that ethanol decomposition takes place. According to the authors, the decomposition of both ethoxy and acetaldehyde species contributes to the formation of methane, hydrogen and CO.

Increasing the temperature to 573 K led to a decrease in the intensities of bands assigned to ν(CO), while the bands at 1547, 1417 and 1342 cm^{-1} increased. Since the bands around 2972–2902 cm^{-1} completely disappeared, the increases observed in the intensities of the bands located at 1547, 1417 and 1342 cm^{-1} are likely attributed to the formation of carbonate species.

At 673 K, the intensities of bands assigned to acetate and/or carbonate species and those of adsorbed CO decreased. At 773 K, the bands corresponding to acetate and/or carbonate species were no longer detected, while the CO remained adsorbed on metal surface. In comparing the results with the TPD data, it is evident that the formation of CO and methane above 500 K detected in TPD profiles of 1.5%Pt/CeO_2 catalyst is consistent with acetate decomposition as observed in the DRIFTS experiment. In addition, as observed for TPD of ethanol, the absence of CO_2 could be due to the dissociation of CO_2 on oxygen vacancies of the ceria support.

3.4.3. DRIFTS analysis under ethanol + water mixture at different temperatures

Fig. 7 shows the DRIFTS spectra of unpromoted CeO_2 under the reaction mixture containing ethanol and water obtained at different temperatures. The spectrum at room temperature exhibits the same bands as observed during DRIFTS analysis after ethanol adsorption (Fig. 5): ethoxy species (1057 and 1101 cm^{-1}); acetate species (1319, 1425 and 1556 cm^{-1}) and both ethoxy and acetate species (2974 and 2881 cm^{-1}). In this case, a new band is detected at around 1626 cm^{-1}, which is attributed to the ν(CO) vibrational mode of acetyl species [39,40]. This intermediate stems from hydrogen elimination of the adsorbed acetaldehyde.

When the sample was heated to 373 K, no significant changes were observed in the DRIFTS spectra. However, increasing temperature to 473 K resulted in a significant increase in the band intensities of acetate species and a decrease in those assigned to ethoxy species. In addition, the bands corresponding to acetyl species disappeared.

At 573 K, the bands of ethoxy species were no longer detected, while the intensities of acetate species bands increased and a band associated to hydrogen carbonate species was also observed at 1612 cm^{-1}.

Above 573 K, the bands assigned to acetate species and hydrogen carbonate species slightly decreased, but both species are still present at 773 K. Moreover, the gas phase CO_2 was also detected at 773 K (2324 and 2364 cm^{-1}).

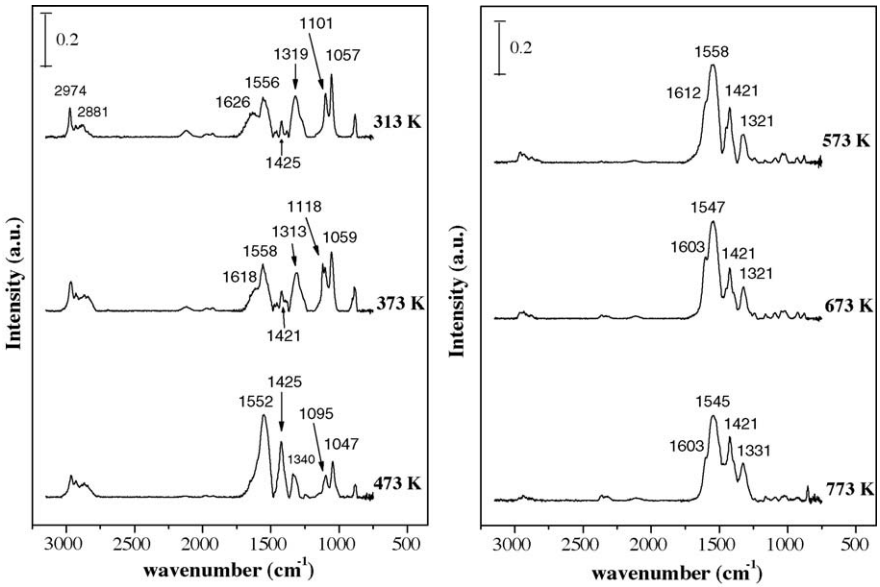

Fig. 7. DRIFTS spectra obtained over unpromoted CeO_2 at different temperatures and under the reaction mixture containing ethanol and water (water/ethanol ratio = 2.0).

The DRIFTS spectra of 1.5%Pt/CeO_2 support recorded during co-feeding of the ethanol + water mixture at different temperatures are presented in Fig. 8. At room temperature, the assignments of the IR bands observed were similar to those reported previously for DRIFTS of ethanol desorption (Fig. 6). However, besides the bands corresponding to ethoxy species, acetate species and linearly adsorbed CO, there is a band related to acetyl species.

At 373 K, the intensities of the bands assigned to adsorb CO on Pt particles increased while those assigned to ethoxy and acetyl species diminished. Furthermore, no significant changes in the intensity of the bands assigned to acetate species were observed and the band corresponding to acetaldehyde (1693 cm^{-1}) may be detected [32,39,40]. These results suggest that the ethoxy and dehydrogenated species were decomposed at low temperatures.

When the sample was heated to 473 K, the bands of acetate species, acetaldehyde and adsorbed CO increased. In addition, the bands related to ethoxy species significantly decreased.

Increasing temperature to 573 K resulted in an increase of the intensity of the bands related to acetate species with a significant decreased in the band corresponding to acetaldehyde. It was also observed that the bands of ethoxy species disappeared, the intensity of the CO band remained unchanged and gas phase CO_2 was clearly present (2324 and 2368 cm^{-1}).

Above 573 K, the intensities of bands characteristic of acetate species and adsorbed CO on Pt decreased. In addition, the presence of carbonate species should be considered, since the bands around 2978–2889 cm^{-1} are no longer detected.

A comparison between the results obtained for DRIFTS experiments under ethanol + water mixture over unpromoted CeO_2 (Fig. 7) and 1.5%Pt/CeO_2 catalyst (Fig. 8) reveal that there are significant differences in the relative intensities of the bands corresponding to each species. Significant amounts of acetate and carbonate species were still detected over unpromoted CeO_2 at high temperatures, in contrast to the results observed for 1.5%Pt/

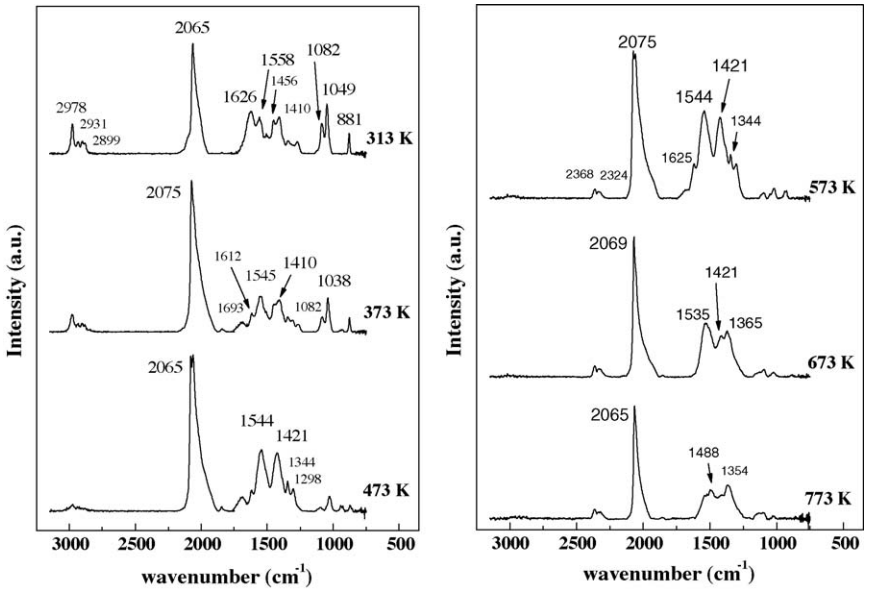

Fig. 8. DRIFTS spectra obtained over 1.5%Pt/CeO_2 catalyst at different temperatures and under the reaction mixture containing ethanol and water (water/ethanol ratio = 2.0).

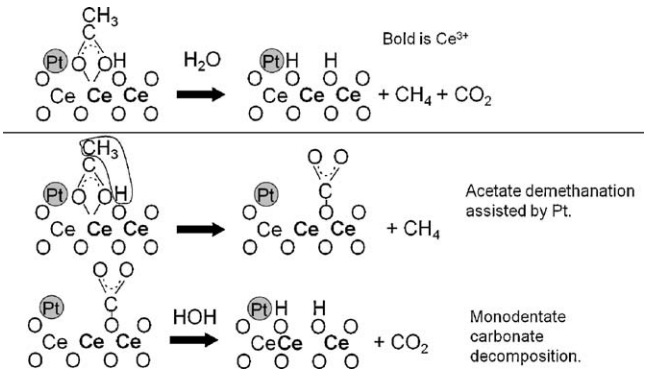

Scheme 3. Forward acetate decomposition.

CeO_2 catalyst. These results indicate that the presence of the metal promotes acetate decomposition at high temperature, which likely occurs at the metal–support interface, as described by the mechanism previously proposed by de Lima et al. [26,27]. This may explain the high selectivities to methane and CO_2 observed initially during steam reforming of ethanol at 773 K for the 1.5%Pt/CeO_2 catalyst (Fig. 2b).

de Lima et al. [26] studied the catalytic performance of a Pt/$CeZrO_2$ catalyst for ethanol decomposition, steam reforming, partial oxidation and oxidative steam reforming of ethanol. The reaction mechanisms were proposed based upon results obtained from TPD of ethanol and in situ DRIFTS analyses carried out under different reaction conditions (DRIFTS of ethanol desorption; DRIFTS under pure ethanol flow and DRIFTS under ethanol + water mixture). Ethanol dissociatively adsorbs to generate ethoxy species and adsorbed H (as a bridging –OH group). The catalytic decomposition of ethoxy species may follow different pathways: (i) decomposition to CO, CH_4, and H_2 or (ii) dehydrogenation to acetaldehyde and acetyl species. The dehydrogenated species may in turn undergo support-induced oxidation to acetate species, with either surface O* or –OH* supplying the O required. As a result, adding co-fed water-promoted acetate species formation. As an added benefit, water also aided the acetaldehyde and acetate decomposition reactions to methane and carbonate, which decomposes to CO_2. This is known as forward acetate decomposition (Scheme 3), and is similar to forward formate decomposition previously proposed [10], which evolves CO_2 and H_2 instead of the reverse decomposition. The reverse decomposition occurs thermally in the absence of H_2O to yield primarily CO and adsorbed H_2O (i.e., as bridging –OH groups). With forward acetate decomposition, the analog of H_2 (forward formate decomposition) is methane. It is important to note that CO is likely produced as a secondary product by reaction of the CO_2 with vacancies, or via an alternate reverse shift mechanism. Both acetate demethanation and CO_2 conversion steps are likely promoted by the interface between the oxide and the Pt, in line with de Lima et al. [26,27].

3.5. Catalyst deactivation during steam reforming of ethanol

The results obtained during continuous steam reforming of ethanol showed that the presence of the metal significantly decreased the stability of the sample. Several authors [14,18,26,27,32] also observed a significant deactivation of supported metal catalysts during steam reforming of ethanol. According to Erdohelyi et al. [14], the catalytic deactivation during steam reforming of ethanol was due to an inhibiting effect caused by surface acetate species. Platon et al. [18] studied the deactivation of $Rh/Ce_{0.8}Zr_{0.2}O_2$ catalysts during low temperature ethanol steam reforming, using transmission electron microscopy (TEM), thermogravimetric analysis (TGA) and TPO analysis. The results did not reveal any significant metal particle sintering or carbon deposits. However, an important buildup of carbonaceous intermediates was observed, which may be a contributing factor in the deactivation of the catalyst. These carbonaceous intermediates were less stable at higher reaction temperatures. Among different reaction intermediates, acetone and ethene were the main ones suggested to be responsible for catalyst deactivation.

Recently, de Lima et al. [26] have studied the performance of Pt/$CeZrO_2$ catalyst during steam reforming of ethanol at 773 K. They also observed that Pt/$CeZrO_2$ catalyst significantly deactivated during the reaction and that this deactivation was followed by an increase of acetaldehyde selectivity. TPO experiments performed after reaction, DRIFTS results and an analysis of the product distributions indicated that the catalyst deactivation could be linked to an increasing surface coverage of acetate intermediates with time on stream.

In this work, it was also detected that the decrease in the ethanol conversion over 1.5%Pt/CeO_2 catalyst was followed by an increase in the acetaldehyde selectivity. In addition, DRIFTS experiments performed under reaction conditions at different temperatures revealed that the coverage of the catalyst surface by acetate species was higher over unpromoted CeO_2 at 773 K, indicating that the presence of the metal increased the turnover rate of acetate species, leading to lower steady state coverage.

Then, in order to determine the nature of the surface species formed during the reaction on 1.5%Pt/CeO_2, DRIFTS spectra were recorded during 6 h under a steady flow of the ethanol + water mixture (H_2O/ethanol molar ratio of 2.0) at 773 K (Fig. 9). The DRIFTS spectrum obtained at the beginning of the reaction were similar to the one observed at 773 K in Fig. 8. The presence of the bands at 1508 and 1373 cm^{-1} and the absence of the bands around 2970–2880 cm^{-1} suggest that this sample contains mainly carbonate species. Furthermore, the bands corresponding to adsorbed CO (2062 cm^{-1}) and CO_2 formation (2330 and 2364 cm^{-1}) were also detected over 1.5%Pt/CeO_2 catalyst. During the reaction, the intensities of bands in the wavenumber region between 1300 and 1600 cm^{-1} (i.e., O–C–O stretching region) increased, while those bands around 2970–2880 cm^{-1} (i.e., C–H stretching region) began to develop and then slightly increase with time onstream. This result indicates that the surface population of acetate species increased as a function of time onstream. Moreover, an increase in the bands assigned to acetate species was accompanied by a decrease in the bands corresponding to

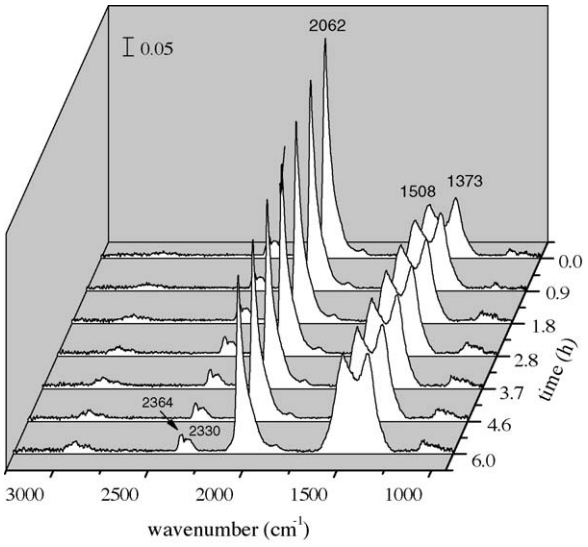

Fig. 9. DRIFTS spectra obtained over 1.5%Pt/CeO_2 at 773 K and under the reaction mixture containing ethanol and water (water/ethanol ratio = 2.0) during 6 h TOS.

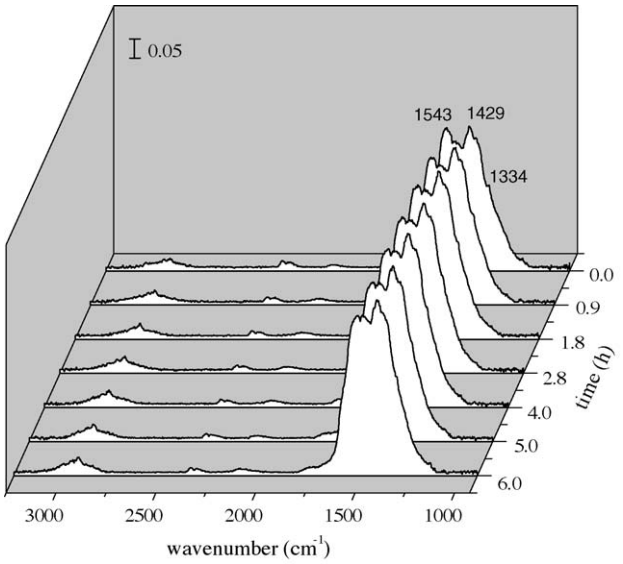

Fig. 10. DRIFTS spectra obtained over unpromoted CeO_2 at 773 K and under the reaction mixture containing ethanol and water (water/ethanol ratio = 2.0) during 6 h TOS.

adsorbed CO. This suggests that the turnover rate for acetate species decomposition decreased during the reaction, leading in turn to increasing acetate coverage on the catalyst surface. According to the reaction mechanism proposed, the acetate species are formed by the oxidation of dehydrogenated species like acetaldehyde and acetyl species. Next, the acetate species are decomposed to methane, CO and/or CO_2. The presence of the metal favors this reaction pathway, since acetate demethanation likely occurs at the metal–support interface. Since the Pt–CO band is decreasing, this points to a loss in Pt active sites as a function of time on stream, thereby inhibiting the acetate demethanation step. In summary, the increasing coverage of acetate species on the catalyst surface with time on stream indicates that the turnover rate for acetate decomposition decreases due to the time dependent loss of the Pt–oxide interaction.

The DRIFTS spectra under the reaction mixture of CeO_2 support obtained at 773 K during 6 h are presented in Fig. 10. The DRIFTS spectrum obtained at the beginning of the reaction was similar to the one observed at 773 K in Fig. 7. The presence of the bands at 1334, 1429, 1543 and around 2970–2880 cm^{-1} indicates that the acetate species is the main species formed over this sample. The acetate species are still present even at high temperature over unpromoted CeO_2, since the metal promoter, which facilitates acetate decomposition, is absent. During the first 3 h of reaction, a slight increase of the intensity of the bands related to acetate species was detected. However, after that, no significant modifications were detected in the DRIFTS spectra of CeO_2.

Therefore, the unpromoted CeO_2 exhibited high surface coverage of adsorbed acetate species at 773 K and did not lose activity during the reaction, which indicates that the accumulation of acetate species on the 1.5%Pt/CeO_2 catalyst surface seems to be symptomatic and not the root cause for the deactivation of the 1.5%Pt/CeO_2 catalyst. Actually, the decomposition of acetate species leads to the formation of CH_x species that recombine with H* adatoms, liberating CH_4. On 1.5%Pt/CeO_2 catalyst, the rate of acetate decomposition may be higher than the rate of desorption of CH_x species as methane, since the presence of the Pt promotes this reaction pathway. The CH_x species formed could in turn lead to the blockage of the Pt–support interface, and thus resulting in catalyst deactivation. Some authors [44] proposed a similar bifunctional mechanism for the steam reforming of acetic acid over Pt/ZrO_2 catalyst. According to them, the catalyst deactivates when the boundary sites between Pt and zirconia are blocked by CH_x residues. In the case of the CeO_2 support, it appears that there may be a proper balance between the rate of acetate decomposition and the rate of desorption of CH_x species which may promote catalyst stability.

Nevertheless, 1.5%Pt/CeO_2 catalyst should exhibit a constant ethanol conversion level of 60–70% even if there is an accumulation of CH_x species on Pt–oxide interface, since this is the conversion level observed for unpromoted CeO_2 after 6 h TOS. However, the ethanol decreased to 10% after 6 h TOS over 1.5Pt%/CeO_2 catalyst. This suggests that the accumulation of CH_x species also spreads over CeO_2 support.

Therefore, CeO_2 is a promising catalyst for steam reforming since it produces H_2 with very low CO content and no significant carbon deposition is formed. As a result, the need for a shift reactor may not be necessary, since the reformate could conceivably be fed directly to the PROX cleanup system. However, the presence of a significant amount of acetaldehyde in the hydrogen rich stream (around 3–5%) demands that the PROX catalyst be designed to simultaneously remove CO and acetaldehyde.

3.6. Preferential CO oxidation (PROX) in the presence of hydrogen using Pt/CeO_2 catalysts

Pt-based catalysts are among the most studied for the PROX reaction. Indeed, many supports, like Al_2O_3 [45,46], SiO_2 [45], CeO_2 [46], activated carbon [47] and also the association with others metals like Fe, Mn, Nb and Co [45,46] have been considered. Recent work published by Park et al. [28] provides an overview of the performance of different catalytic systems, where even very simple systems like Pt/Al_2O_3 and Pt/CeO_2 are indicated to be able to completely eliminate CO from the hydrogen stream. In this work, the performance of a Pt/CeO_2 catalysts for the conversion of low concentrations of CO in the presence of acetaldehyde was studied. Pt/Al_2O_3 was used as a reference.

The activity of the different x%Pt/CeO_2 and 1.5%Pt/Al_2O_3 catalysts was initially examined by calculating the reaction rate under differential conditions at 348 K (Fig. 11). Increasing Pt content increases the reaction rate of CO removal, reaching a maximum for 1.5%Pt/CeO_2 and then decreasing at higher Pt concentration. A comparison between the reaction rate of 1.5%Pt/CeO_2 and 1.5%Pt/Al_2O_3 catalysts reveals that the ceria supported catalyst is more active. Therefore, ceria supported catalyst containing 1.5%Pt was selected as the catalyst for the tests of CO removal. 1.5%Pt/Al_2O_3 catalyst was also used as a reference.

Fig. 12 shows the CO outlet concentration and H_2 conversion versus temperature during PROX reaction over 1.5%Pt/CeO_2 and

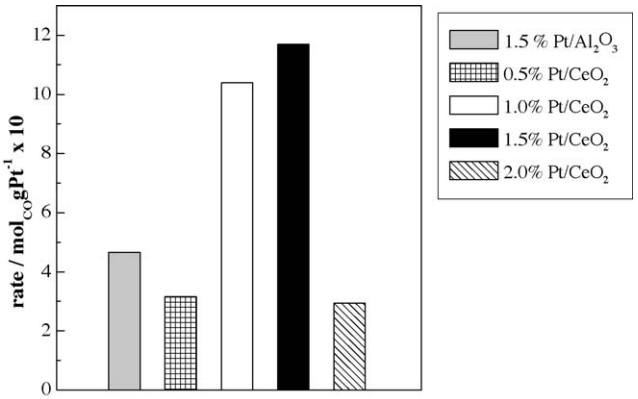

Fig. 11. CO reaction rate over x%Pt/CeO_2 (x = 0.5, 1.0, 1.5 and 2.0) and 1.5%Pt/Al_2O_3 catalysts ($T_{reaction}$ = 348 K; $m_{catal.}$ = 8 mg; flow rate = 60 mL/min; reactant mixture composed by 50% H_2, 200 ppm CO, 2% O_2 and balanced with N_2).

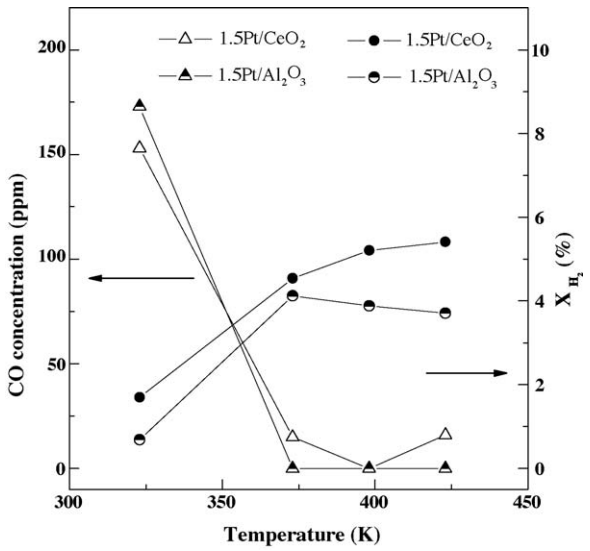

Fig. 12. CO outlet concentration and H_2 conversion during the PROX reaction over 1.5%Pt/CeO_2 and 1.5%Pt/Al_2O_3 catalysts (flow rate = 60 mL/min; $m_{catal.}$ = 15 mg; reactant mixture composed by 50% H_2, 200 ppm CO, 2% O_2 balanced with N_2).

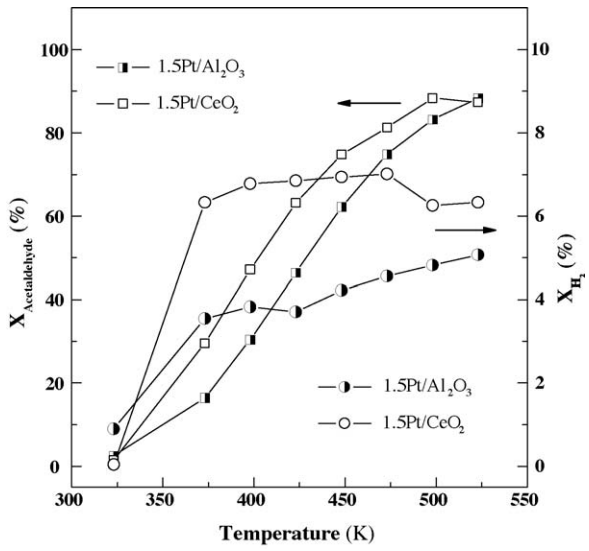

Fig. 13. Acetaldehyde and H_2 conversions ($X_{Acetaldehyde}$ and X_{H_2}, respectively) during the PROX reaction over 1.5%Pt/CeO_2 and 1.5%Pt/Al_2O_3 catalysts (flow rate = 60 mL/min; $m_{catal.}$ = 15 mg; reactant mixture composed by 50% H_2, 200 ppm CO, 2% O_2 and 1% of acetaldehyde balanced with N_2).

1.5%Pt/Al_2O_3 catalyst. Both catalysts eliminate completely the CO (<10 ppm) from the hydrogen stream at around 400 K. In addition, hydrogen consumption does increase as the temperature increases and is slightly higher for 1.5%Pt/CeO_2 catalyst in the entire temperature region.

3.7. The CO oxidation in the presence of hydrogen and acetaldehyde

Fig. 13 shows the acetaldehyde and hydrogen conversion of 1.5%Pt/CeO_2 and 1.5%Pt/Al_2O_3, respectively. Regardless of the catalyst type, the acetaldehyde conversion increases whereas the hydrogen conversion remains constant as temperature increases. In addition, 1.5%Pt/CeO_2 was the most active. A comparison with Fig. 11 reveals that the H_2 consumption rates over both catalysts were not significantly affected by the presence of acetaldehyde.

The CO content at the outlet of the reactor as a function of reaction temperature during the PROX reaction in the presence of acetaldehyde is shown in Fig. 14. The CO concentration was reduced from 200 ppm (inlet composition) to less than 10 ppm at temperatures between 425 and 450 K over the 1.5%Pt/CeO_2 catalyst (Fig. 14a). However, the CO levels begin to increase above 450 K, reaching values of around 680 ppm at 525 K, which is much higher than the CO composition of the feed. This result suggests that CO is somehow being produced during the reaction.

The curve of CO concentration versus reaction temperature for 1.5%Pt/Al_2O_3 catalyst (Fig. 14b) was similar to the one observed for 1.5%Pt/CeO_2 (Fig. 14a). The CO concentration decreases as temperature increases, reaching a minimum at 373 K and then increases for higher temperatures. The lowest CO concentration is around 36 ppm, which is higher than those values observed for 1.5%Pt/CeO_2. These results can be associated with the higher activity of the 1.5%Pt/CeO_2 catalyst. At high temperatures, this catalyst also generated CO. Indeed, CO concentration at 523 K is 50% higher relative to the CO composition of the feed.

For 1.5%Pt/CeO_2 catalyst (Fig. 14a), methane, carbon dioxide and ethanol are the main products formed during the PROX reaction in the presence of acetaldehyde. Increasing temperature, the selectivity to methane increases continuously whereas the selectivity to ethanol remains approximately constant from 373 to 525 K. The selectivity towards CO_2 increases as temperature increases, achieving a maximum around 400 K and then, it drops, leveling off at 425 K. For 1.5%Pt/Al_2O_3 catalyst (Fig. 14b), the methane and CO_2 selectivities increase and level off at around 373 K, while ethanol was never detected in the temperature region studied.

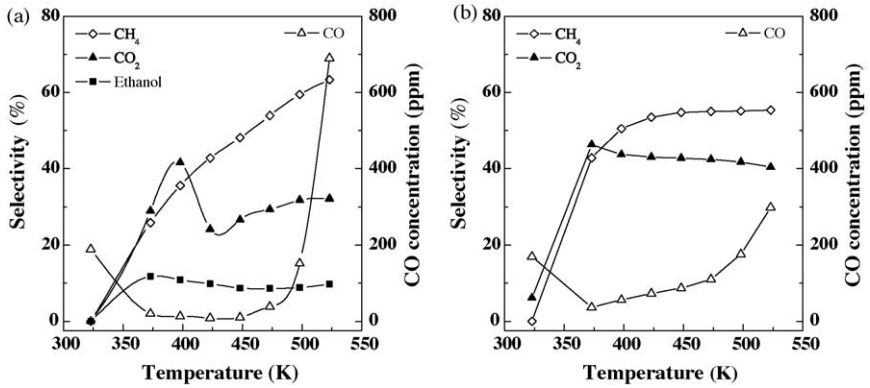

Fig. 14. Selectivity towards CH_4, CO_2 and ethanol (S_{CH_4}, S_{CO_2} and $S_{ethanol}$, respectively) and the CO outlet concentration (ppm) during the PROX reaction over (a) 1.5%Pt/CeO_2 and (b) 1.5%Pt/Al_2O_3 catalysts (flow rate = 60 mL/min; $m_{catal.}$ = 15 mg; reactant mixture composed by 50% H_2, 200 ppm CO, 2% O_2 and 1% of acetaldehyde balanced with N_2).

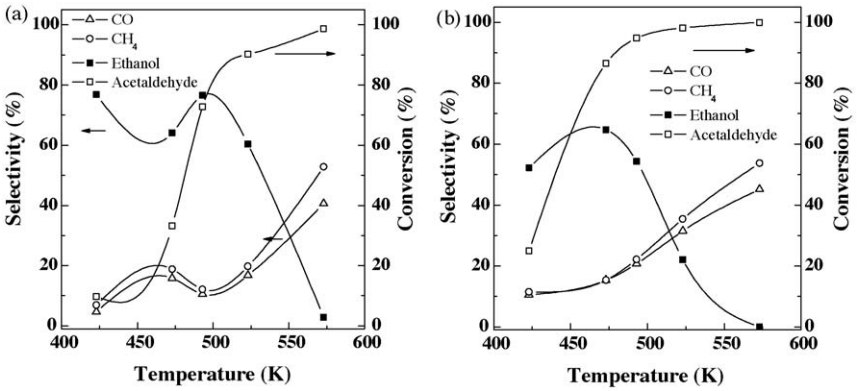

Fig. 15. Acetaldehyde conversion ($X_{Acetaldehyde}$) and selectivity towards CH_4, CO and ethanol (S_{CH_4}, S_{CO} and $S_{ethanol}$, respectively) during the reaction of acetaldehyde in the absence of oxygen over (a) 1.5%Pt/CeO_2 and (b) 1.5%Pt/Al_2O_3 catalysts (flow rate = 60 mL/min; $m_{catal.}$ = 200 mg; reactant mixture composed by 61% H_2 and 3.7% of acetaldehyde balanced with N_2).

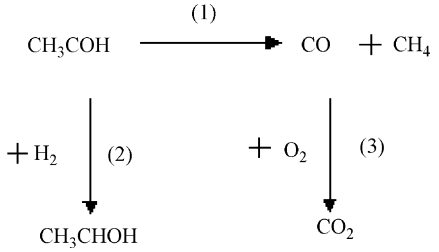

Scheme 4. Steps for the PROX reaction in the presence of acetaldehyde: (1) acetaldehyde decomposition to CO and methane; (2) acetaldehyde hydrogenation to ethanol; and (3) oxidation of CO to CO_2.

In order to better describe the behavior of acetaldehyde in the presence of hydrogen, some experiments were carried out by using a feed without oxygen (Fig. 15a and b). For both catalysts, the main products obtained were methane, CO and ethanol. Trace amounts of ethyl acetate and acetal were also detected in the low temperature region whereas a small quantity of ethane was detected at high temperatures. As the reaction temperature increased, the acetaldehyde conversion and the selectivity to CO and methane increased whereas the selectivity towards ethanol decreased. It is noteworthy that the CO and methane selectivity are very similar, for both catalysts, suggesting that they are generated by the same reaction. Indeed, the decomposition or decarbonylation of acetaldehyde leading to methane and carbon monoxide is thermodynamically feasible under these reaction conditions ($\Delta H_{298K} = -54.4$ kJ mol^{-1}). This reaction is described in the literature for some homogenous catalysts and also for nickel and palladium based heterogeneous catalysts [48,49]. Therefore, two main reactions may be considered in this case, the acetaldehyde hydrogenation to ethanol and the acetaldehyde decomposition to CO and methane.

Therefore, the high CO concentration observed at high temperatures during the PROX reaction in the presence of acetaldehyde (Fig. 14a and b) may be attributed to acetaldehyde decomposition. In addition, the CO_2 produced comes not only from the CO present in the feed but mainly from the CO formed during the acetaldehyde decomposition.

It is noteworthy that the CO_2 selectivity reaches a maximum at 397 K and then decreases during the PROX reaction in the presence of acetaldehyde over 1.5%Pt/CeO_2 (Fig. 14a). In order to understand this behavior, the reaction was stopped at 523 K and the catalyst was heated under N_2. At 773 K, the evolution of large amount of CO_2, showing that carbonates were present on the catalyst surface. This result suggests that the decrease in CO_2 selectivity may be attributed to the reaction between CO_2 and CeO_2 and the formation of carbonates [50].

Comparing the acetaldehyde conversion in the presence and absence of oxygen, at temperatures above 398 K (Figs. 14 and 15), it is clear that oxygen favored the acetaldehyde decomposition reaction. In fact, the CO oxidation during the PROX reaction shifts the equilibrium of the acetaldehyde decomposition reaction.

A comparison between the ethanol selectivity in Fig. 15a and b (the acetaldehyde reaction without O_2) suggests that 1.5%Pt/CeO_2 is much more active for the hydrogenation reaction than 1.5%Pt/Al_2O_3. This result may explain the absence of ethanol formation over 1.5%Pt/Al_2O_3 during the PROX reaction in the presence of acetaldehyde.

In addition, from Fig. 14a and b, it is clear that the selectivity to methane is always higher than the selectivity to CO_2, suggesting that methane might also be synthesized by CO or CO_2 methanation. This result is now under investigation.

Taking into account these results, the following reaction mechanism could be proposed to explain the PROX reaction in the presence of acetaldehyde (Scheme 4): (1) acetaldehyde decomposition to CO and methane; (2) acetaldehyde hydrogenation to ethanol; and (3) oxidation of CO to CO_2.

4. Conclusions

While 1.5%Pt/CeO_2 was found to be a significantly more active catalyst than ceria alone for ethanol steam reforming, the catalyst was found to deactivate very rapidly. The mechanism of ethanol decomposition was probed by TPD and DRIFTS, while the mechanism of ethanol steam reforming was monitored by steady state DRIFTS. The mechanism of ethanol steam reforming was found to involve six main steps, including (1) dissociation of ethanol on partially reduced ceria to ethoxy species and a bridging OH group; (2) dehydrogenation of the ethoxy species to acetaldehyde; (3) oxidation of acetaldehyde by mobile bridging OH groups to acetate; (4) water-promoted acetate demethanation to carbonate; and (5) carbonate decomposition to CO_2 and, presumably (6) methane conversion steps. Pt was found to promote the hydrogen transfer and acetate demethanation steps. CO_2 produced was also converted by a secondary reaction to CO. Steady state DRIFTS results indicated that there was a loss in the Pt active site density with time, probably by the buildup of carbon-containing species at the boundary between Pt and ceria, shutting down not only the metal-promoted pathway, but causing enough carbon overlayers to bring the conversion level well below that of unpromoted ceria. Since Pt assisted in demethanating acetate, loss of Pt sites caused not only the Pt–CO band to diminish, but the

steady state inventory of acetate to increase (i.e., due to a lower turnover rate).

This contribution reports, for the first time, H_2 purification in the presence of acetaldehyde since it was found to be an important by-product from ethanol steam reforming over unpromoted CeO_2. Methane, carbon dioxide and ethanol were observed to be the main products. The steps for the PROX reaction in the presence of acetaldehyde included: (1) acetaldehyde decomposition to CO and methane; (2) acetaldehyde hydrogenation to ethanol; and (3) oxidation of CO to CO_2. The CO_2 produced by the PROX reaction was in some cases 8 times higher than the inlet CO concentration. As a result, it was evident that CO consumption generated by the oxidation shifted the equilibrium of the acetaldehyde decomposition reaction to favor product. The presence of this aldehyde in the H_2 stream, even at low CO concentration, makes the H_2 purification step more challenging.

Acknowledgements

This work received financial support of CTENERG/FINEP-01.04.0525.00. CAER acknowledges the Commonwealth of Kentucky for financial support.

References

[1] J.M. Ogden, Int. J. Hydrogen Energy 24 (1999) 709.
[2] P. Forsberg, M. Karlström, Int. J. Hydrogen Energy 32 (2007) 647.
[3] J.R. Rostrup-Nielsen, Catal. Today 106 (2005) 293.
[4] P. Ferreira-Aparício, M.J. Benito, Catal. Rev. 47 (2005) 491.
[5] J.H. Hirschenhofer, D.B. Atauffer, R.R. Engleman, M.G. Klent, Fuel Cell Handbook, 4th ed., 1998.
[6] P.D. Vaidya, A.E. Rodrigues, Ind. Eng. Chem. Res. 45 (2006) 6614.
[7] A. Haryanto, S. Fernando, N. Murali, S. Adhikari, Energy Fuels 19 (2005) 2098.
[8] H. Song, L. Zhang, R.B. Watson, D. Braden, U.S. Ozkan, Catal. Today 129 (2007) 346.
[9] R.M. Navarro, M.C. Alvarez-Galvan, M.C. Sanchez-Sanchez, F. Rosa, J.L.G. Fierro, Appl. Catal. B 55 (2004) 223.
[10] G. Jacobs, R.A. Keogh, B.H. Davis, J. Catal. 245 (2007) 326.
[11] L.P.R. Profeti, E.A. Ticianelli, E.M. Assaf, J. Power Sources 175 (2008) 482.
[12] M. Veronica, B. Graciela, A. Norma, L. Miguel, Chem. Eng. J. 138 (2008) 602.
[13] A.N. Fatsikostas, X.E. Verykios, J. Catal. 225 (2004) 439.
[14] A. Erdohelyi, J. Raskó, T. Kecskés, M. Tóth, M. Dömök, K. Baán, Catal. Today 116 (2006) 367.
[15] V. Fierro, V. Klouz, O. Akdim, C. Mirodatos, Catal. Today 75 (2002) 141.
[16] J.M. Guil, N. Homs, J. Llorca, P.R. de la Piscina, J. Phys. Chem. B 109 (2005) 10813.
[17] J.C. Vargas, S. Libs, A.C. Roger, A. Kiennemann, Catal. Today 107 (2005) 417.
[18] A. Platon, H.S. Roh, D.L. King, Y. Wang, Top. Catal. 46 (2007) 374.
[19] N. Laosiripojana, S. Assabumrungrat, Appl. Catal. B 66 (2006) 29180.
[20] T. Nishiguchi, T. Matsumoto, H. Kanai, K. Utani, Y. Matsumurab, W.-J. Shenc, S. Imamura, Appl. Catal. A 279 (2005) 273.
[21] J. Llorca, N. Homs, P.R. de la Piscina, J. Catal. 227 (2004) 556.
[22] J. Llorca, P.R. de la Piscina, J. Sales, N. Homs, Chem. Commun. (2001) 641.
[23] W. Cai, F. Wanga, E. Zhan, A.C. Van Veen, C. Mirodatos, W. Shen, J. Catal. 257 (2008) 96.
[24] J. Kugai, V. Subramani, C. Song, M.H. Engelhard, Y.H. Chin, J. Catal. 238 (2006) 430.
[25] H. Roh, A. Platon, Y. Wang, D.L. King, Catal. Lett. 110 (2006) 1.
[26] S.M. de Lima, I.O. da Cruz, G. Jacobs, B.H. Davis, L.V. Mattos, F.B. Noronha, J. Catal. 257 (2008) 356.
[27] S.M. de Lima, A.M. Silva, I.O. da Cruz, G. Jacobs, B.H. Davis, L.V. Mattos, F.B. Noronha, Catal. Today 138 (2008) 162–168.
[28] E.D. Park, D. Lee, H.C. Lee, Catal. Today 139 (2009) 280–290.
[29] M. Boudart, Adv. Catal. 20 (1969) 153.
[30] P. Pantu, G.R. Gavalas, Appl. Catal. A 223 (2002) 253.
[31] F.B. Passos, E.R. de Oliveira, L.V. Mattos, F.B. Noronha, Catal. Today 101 (2005) 23.
[32] M. Dömök, M. Tóth, J. Raskó, A. Erdohelyi, Appl. Catal. B 69 (2007) 262.
[33] L.V. Mattos, F.B. Noronha, J. Catal. 233 (2005) 453.
[34] A. Yee, S.J. Morrison, H. Idriss, J. Catal. 186 (1999) 279.
[35] M.A.S. Baldanza, L.F. de Mello, A. Vannice, F.B. Noronha, M. Schmal, J. Catal. 192 (2000) 64.
[36] E.M. Cordi, J.L. Falconer, J. Catal. 162 (1996) 104.
[37] L.F. de Mello, F.B. Noronha, M. Schmal, J. Catal. 220 (2003) 358.
[38] A. Yee, S.J. Morrison, H. Idriss, J. Catal. 191 (2000) 30.
[39] H. Idriss, C. Diagne, J.P. Hindermann, A. Kiennemann, M.A. Barteau, J. Catal. 155 (1995) 219.
[40] R. Shekhar, M.A. Barteau, R.V. Plank, J.M. Vohs, J. Phys. Chem. B 101 (1997) 7939.
[41] P.V. Menacherry, G.L. Haller, J. Catal. 177 (1998) 175.
[42] H. Bischoff, N.I. Jaeger, G. Schulz-Ekloff, L. Kubelkova, J. Mol. Catal. A: Chem. 80 (1993) 95.
[43] M. Primet, J. Catal. 88 (1984) 273.
[44] K. Takanabe, K-Ichi. Aika, K. Inazu, T. Baba, K. Seshan, L. Lefferts, J. Catal. 243 (2006) 263.
[45] S.-H. Oh, R.M. Sinkevitch, J. Catal. 142 (1993) 254.
[46] F. Mariño, C. Descorme, D. Duprez, Appl. Catal. B 54 (2004) 59.
[47] E. Şimşek, Ş Özkara, A.E. Aksoylu, Z.I. Önsan, Appl. Catal. A 316 (2007) 169.
[48] J.-R. Roy, M.-A. Laliberté, S. Lavoie, M. Castonguay, P.H. McBreen, Surf. Sci. 578 (2005) 43.
[49] M. Bowker, R. Holroyd, N. Perkins, J. Bhantoo, J. Counsell, A. Carley, C. Morgan, Surf. Sci. 601 (2007) 3651.
[50] L.G. Appel, J.G. Eon, M. Schmal, Catal. Lett. 56 (1998) 1999.